Rheodielectric study of transformer-oil-based ferrofluids

Katarina Paulovicova,[1] Michal Rajnak,[1,2] Jana Tothova,[2] Bystrik Dolnik,[2] Milan Timko,[1] and Peter Kopcansky[1]
[1]*Institute of Experimental Physics SAS, Watsonova 47, 04001 Košice, Slovakia*
[2]*Faculty of Electrical Engineering and Informatics, Technical University of Košice, Letná 9, 04200 Košice, Slovakia*

(Received 4 February 2025; accepted 25 March 2025; published 8 April 2025)

The rheological properties of nonpolar ferrofluids have been often studied under the action of an external magnetic or electric field. In this paper, we approach the problem conversely, and we aim to answer whether the ferrofluid shear flow affects the dielectric response. The ferrofluids are based on transformer oil and iron oxide nanoparticles stabilized with oleic acid. Basic physical characterization of the ferrofluids with three different nanoparticle concentrations is followed by experimental investigation of flow curves. Newtonian behavior of the ferrofluids is confirmed. The key experiment of this study consists of complex dielectric permittivity measurements in the frequency range from 20 Hz to 100 kHz at three different temperatures. In these measurements, the ferrofluids are sandwiched between two disk electrodes of a modular rheometer under the shear rates of 0, 10, 100, 500, and 1000 s^{-1}. It is found that the low-frequency dielectric spectra of the ferrofluids exhibit a remarkable conductivity contribution leading to electrode polarization. Additional measurements of electrical conductivity and qualitative analysis of charge mobility in the ferrofluids are provided to understand the low-frequency dielectric relaxation. The results reveal that the slow dielectric relaxation is shear rate independent. The low-frequency dielectric spectra measured under the various shear rates exhibit constant behavior. The electric charge migrates across the shear flow velocity in the shear rate direction and the given rheological conditions do not affect its behavior. It is concluded that the electrical forces dominate the charge motion in the ferrofluids over the shear forces. The finding of the stable dielectric response of ferrofluids under the shear flow conditions supports the application of ferrofluids as dielectric media in electrical equipment with the presence of forced or natural convection.

DOI: 10.1103/PhysRevE.111.045403

I. INTRODUCTION

Magnetic nanofluids, also called ferrofluids, are colloidal suspensions of magnetic nanoparticles in aqueous or nonaqueous liquids [1]. Owing to their strong magnetic properties, they find various applications, including heat transfer, magnetic resonance imaging, dynamic loudspeakers, and others [2]. Even though the ferrofluids have been of scientific interest already for several decades, there are still new research opportunities regarding the methods of ferrofluid preparation, along the study of physical properties and applications of ferrofluids in biomedicine and engineering fields [3]. As the ferrofluids are susceptible to external magnetic fields, various properties and phenomena have been investigated experimentally and theoretically in dependence on a magnetic field. For instance, the translational dynamics of maghemite nanoparticles in decane was found to be dependent on magnetic field, as observed by dynamic light scattering study [4]. An external magnetic field can also reduce or enhance the adhesive strength of a high-viscosity ferrofluid [5]. In literature, one finds that it is the viscosity that has been intensively studied on various types of ferrofluids because it plays a crucial role in ferrofluid applications. It is well-known that the rheological behavior of a typical ferrofluid is essentially Newtonian. However, in magnetic fields, the ferrofluids' viscosity depends not only on the magnitude of the magnetic field but also on its relative orientation to the flow geometry [6]. This phenomenon is known as anisotropy of the magnetoviscous effect, and it is related to the underlying change in the microstructure of ferrofluids [7]. It has been studied experimentally [8] and several theoretical models of the viscoelastic properties of ferrofluids considering various structural changes in magnetic fields have been proposed [9–11]. A magneto-viscosity expression coming from the effective-field method and shear-thinning non-Newtonian behavior was described by Weng *et al.* [12]. The magnetorheological response of ferrofluids is remarkably given by the nanoparticle morphology [13], and the magnetoviscous effect can be enhanced by increasing the magnetic field inclination [14]. It was shown that the friction between the anisotropic particles decreases with an increase in nanoparticle concentration [15]. Recently, a hysteresis effect between viscosity and magnetic field was studied and inverse associations between them were attributed to the combined influence of thixotropy and magnetic field [16]. The ferrofluids undergoing unsteady shear flows in the presence of a magnetic field become viscoelastic liquids [17]. Among other fascinating physical phenomena revealed in relation to the ferrofluid viscosity one can mention the rotational viscosity and negative viscosity effects [18,19]. Nonlinear rheology was applied in the study of microstructural changes in magnetically modified crude oils [20].

It is therefore evident that the rheological behavior of ferrofluids is intensively studied under the action of a magnetic field. However, there is a class of ferrofluids based on transformer oils investigated for electrical engineering applications, mostly as smart insulating and cooling liquids [21–24]. In this field, the ferrofluids' physical properties must

be studied also in electric fields. It was found that, analogously to the magnetic field effect, the electric field also induces structural changes in ferrofluids [25,26]. As a result, the ferrofluid's viscosity increases with increasing electric field [27]. Thus, the electric field influences the flow behavior of the ferrofluids. But does it work vice versa? Can the ferrofluid flow influence the electric behavior of ferrofluids? Does the ferrofluid flow influence the dielectric response of the ferrofluid constituents and their interface with electrodes? It is important to address that problem especially when considering the ferrofluids for applications in equipment like electrical transformers. There, the ferrofluid undergoes natural or even forced convection and simultaneously is exposed to an alternating electric field. To answer the above questions, one must undertake an experimental research on the rheodielectric response of ferrofluids. To the best of our knowledge, such a study has not been reported yet.

On the other hand, the topic of the dielectric response of ferrofluids is of immense scientific interest. Special attention has been paid to a low frequency dielectric response of ferrofluids exhibiting low-frequency dielectric relaxations [28–30]. For instance, the Schwarz model of electric double-layer polarization was used to explain the low-frequency dielectric relaxation in ferrofluids [31,32]. Recently, a thermal aging study of transformer oil-based ferrofluids found that the effect of electric double-layer polarization disappears after 500 h of thermal aging [33]. Clearly, the dielectric response of ferrofluids is affected by external magnetic fields [34], but it is also evident that the dielectric spectrum of a ferrofluid is controllable by means of a static electric field generated by a direct current (dc) bias voltage [35]. Moreover, the acting DC bias electric field causes the permittivity sign switching at low frequencies [36]. The phenomenon was explained via nanoparticle assembly and conductive percolative paths as key mechanisms leading to the transition from capacitive to inductive reactance. Batalioto *et al.* analyzed an electric response of ferrofluid cells containing different concentrations of magnetic nanoparticles in kerosene, limited by different types of electrodes. Their experimental data are well fitted by a simple model based on lumped elements [37]. The impedance spectroscopy was also used by Batalioto *et al.* to investigate the influence of the free ions and the electrode material on the electric response of a kerosene-based ferrofluid cell with the application of Poisson-Nernst-Planck (PNP) model [38]. They showed that the electric response of the ferrofluid cell at low frequencies (below 10 mHz) can be interpreted by means of the model based on the adsorption of ions from limiting surfaces – the generalized PNP model containing surface capacitance [39]. The free ions considered in their measurements originate from the ferrofluid preparation process, released by the stabilization layer around the magnetic nanoparticles [40]. Another study of the impedance spectra of a kerosene based ferrofluid revealed that even a low sinusoidal voltage of 80 mV can give rise to nonlinear effects at frequencies lower than 100 mHz [41].

While the low-frequency dielectric response of nonpolar ferrofluids in electric, magnetic, and thermal fields has been studied extensively, the effects of applied shear stress on dielectric spectra of ferrofluids have received far less attention. Simultaneous rheology and dielectric experiments are reported rarely. For instance, the rheodielectric technique, which involves the study of the dielectric response of a material in the presence of shear forces, has been applied to determine how shear-induced structural changes alter charge distributions and polarization fluctuations in liquid crystals, polymers or carbon black suspensions [42–45]. Misra *et al.* studied the dielectric behavior of strongly sheared aqueous suspensions of thermoreversible hydrogel poly(*N*-isopropylacrylamide) particles at different temperatures [46]. In ferrofluid research, the rheological and dielectric measurements have been conducted independently, and rheodielectric studies focusing on the low-frequency dielectric response of transformer oil-based ferrofluids under applied strains have not been reported, to the best of our knowledge. In this paper, we attempt to bridge this gap by performing rheodielectric experiments on transformer oil-based ferrofluids with three different nanoparticle concentrations. In this way, we want to find out if there is any effect of the ferrofluid flow on the dielectric response. This question is of importance especially when considering the potential application of ferrofluids as dielectric liquids undergoing natural or forced convection in electrical equipment. The paper is organized as follows. In the following Sec. II, we briefly introduce basic technical terms and definitions used throughout the study. In Sec. III, we describe the studied materials and experimental methods employed in the presented study. The results and discussion are presented in the last Sec. IV.

II. DEFINITION OF BASIC TERMS

In this study, the dielectric spectroscopy method is applied to transformer oil-based ferrofluids under shear flow conditions. The dielectric spectroscopy measures the response of the material under an applied alternating electric field. The external electric field induces displacements of electric charges within the material, resulting in macroscopic polarization of the sample. There are several types of dielectric polarizations, e.g., ionic, interfacial, and atomic polarization [47]. The response from electric charge displacement is often characterized by means of frequency-dependent complex dielectric permittivity given by its real $\varepsilon'(\omega)$ and imaginary $\varepsilon''(\omega)$ component as follows:

$$\varepsilon^*(\omega) = \varepsilon'(\omega) - i\varepsilon''(\omega). \tag{1}$$

The complex permittivity is connected with complex conductivity by a simple relationship

$$\sigma^*(\omega) = i\omega\varepsilon_0\varepsilon^*(\omega), \tag{2}$$

where ε_0 is the vacuum permittivity and $\omega = 2\pi f$ is the angular frequency. The real conductivity is proportional to the imaginary permittivity, while the imaginary conductivity is proportional to the real permittivity

$$\sigma'(\omega) = \omega\varepsilon_0\varepsilon''(\omega), \tag{3}$$

$$\sigma''(\omega) = \omega\varepsilon_0\varepsilon'(\omega). \tag{4}$$

In the simplest case, the dielectric relaxation is of Debye type with a single relaxation time and it is described by the

TABLE I. The selected characteristics of the base insulating oil as provided by the manufacturer.

Properties	Typical values
Density at 15°C (g/cm^3)	0.865
Kinematic viscosity at 20°C (mm^2/s)	22
Kinematic viscosity at 40°C (mm^2/s)	9.3
Pour point (°C)	–45
Flash point (°C)	155
Breakdown voltage (kV)	60
Dielectric dissipation factor at 90°C, at 40 Hz to 60 Hz	0.0006

following formula:

$$\varepsilon^*(\omega) = \varepsilon'(\omega) - i\varepsilon''(\omega) = \varepsilon_\infty + \frac{\Delta\varepsilon}{1 + i\omega\tau}, \tag{5}$$

where τ is the relaxation time and $\Delta\varepsilon$ is called dielectric relaxation strength given as the difference between the permittivity values at a low and a high frequency limit [48].

Herein, we attempt to find out whether the above-listed dielectric parameters reflecting the charge displacement in the ferrofluids are dependent on the applied shear stress or not. The shear stress τ is defined according to the two-plates-model as a shear force divided by a shear area

$$\tau = F/A. \tag{6}$$

The unit is $1\,\mathrm{N/m^2} = 1$ Pa. The shear rate $\dot{\gamma}$ (also deformation rate or shear gradient) is defined as the flow velocity divided by the gap width.

$$\dot{\gamma} = v/h \tag{7}$$

The unit for shear rate is the reciprocal second ($1\,\mathrm{s^{-1}}$). Then, viscosity is defined as the shear stress divided by the shear rate

$$\eta = \tau/\dot{\gamma}. \tag{8}$$

This is the well-known Law of viscosity or Newton's law. η is sometimes termed dynamic viscosity. The unit of viscosity is Pa s [49].

III. MATERIALS AND METHODS

The carrier liquid used in the present study is an inhibited insulating transformer oil MOL TO 40A. It contains naphthenic base oils and additives that inhibit oxidation. The basic physical parameters provided by the manufacturer are listed in Table I.

The transformer oil has been nanofunctionalized by iron oxide magnetic nanoparticles (MNP). The MNP were synthesized by the chemical coprecipitation method, by using iron (II) sulfate heptahydrate ($FeSO_4 \cdot 7H_2O$), iron (III) chloride hexahydrate ($FeCl_3 \cdot 6H_2O$) and ammonium hydroxide solution (NH_4OH). Oleic acid ($C_{17}H_{33}COOH$) was used as a surfactant to stabilize the MNP [50]. All raw materials were of analytical reagent grade without any additional purification. The preparation of the basic ferrofluid consisted

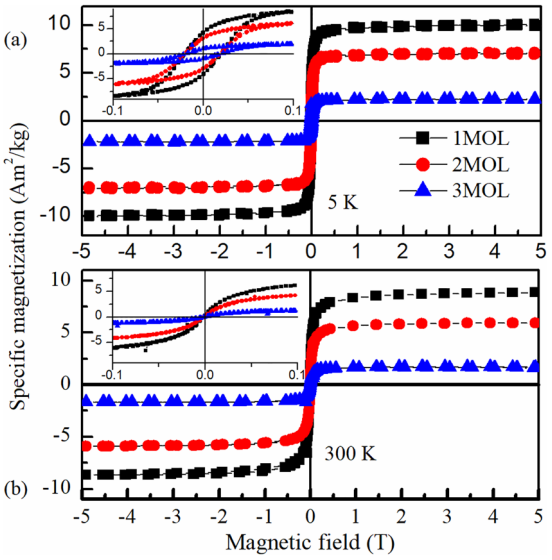

FIG. 1. Specific magnetization curves measured on the ferrofluid samples at 5 K (a) and 300 K (b).

of two steps. First, the MNP were obtained by the chemical coprecipitation of the ferrous and ferric salts in the molar rate 1:2 in an alkali medium at the temperature of 353 K. Then, MNP were sterically stabilized and coated by a single layer of oleic acid at the temperature range (353 − 355) K. The coated MNP with hydrophobic character were dispersed in the transformer oil MOL and a stable suspension without any phase separation and sedimentation was achieved. The basic ferrofluid was finally diluted by the transformer oil MOL and three ferrofluid samples were prepared with the magnetic mass fraction 12%, 8%, and 2%, labeled as MOL1, MOL2, and MOL3, respectively. The magnetic mass fraction was determined as a ratio of the ferrofluid magnetization of saturation to the magnetization of saturation of the powder MNP (73 Am^2/kg). The ferrofluids and MNP powder magnetizations were measured by means of a vibrating sample magnetometer installed on a cryogen-free superconducting magnet system from Cryogenic Limited (UK). The obtained magnetization curves measured at 5 and 300 K temperatures are presented in Figs. 1(a) and 1(b). The magnetizations of saturation at 300 K found for MOL1, MOL2, and MOL3 are 8.9 Am^2/kg, 5.9 Am^2/kg, and 1.7 Am^2/kg, respectively. These values reflect the above-determined magnetic mass fractions. The magnetization curves of all samples exhibit a typical superparamagnetic behavior at 300 K with the characteristic zero hysteresis. This is well visible in the inset of Fig. 1(b). The experimental confirmation of the superparamagnetic state of the ferrofluids at room temperature is crucial for the rheodielectric experiments presented herein. In this state, the MNP are noninteracting, and therefore any MNP structures induced by spontaneous magnetic interactions are not considered to influence the rheological response. On the other hand, the low-temperature magnetization curves show remarkable hysteresis pointing to the blocked state of the MNP magnetic moments [the inset of Fig. 1(a)].

To reveal the temperature area of the transition from the blocked to the superparamagnetic state, we performed

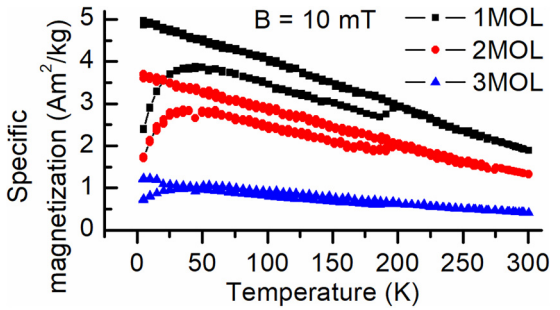

FIG. 2. Specific magnetizations of the ferrofluids measured in zero-field-cooling (ZFC – the lower curves) and field-cooling (FC – the upper curves) regime.

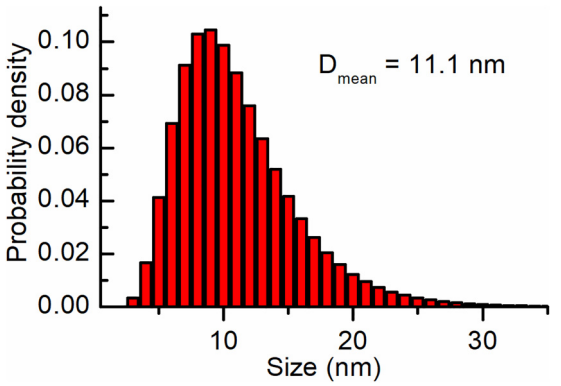

FIG. 3. Particle size distribution function obtained from the measured magnetization curve (1MOL).

the zero-field-cooling (ZFC) and field-cooling (FC) magnetization measurements. The measurements were conducted in a static magnetic field of 10 mT. Figure 2 shows the temperature-dependent behavior of the specific magnetization of the ferrofluid samples. Each ZFC curve (the lower curve) exhibits a shoulder below 50 K temperature. The shoulder is associated with the transition of the magnetic moments from the superparamagnetic to the blocked state. The shoulder shape, instead of a sharp transition, reflects the MNP size distribution, which is connected with the distribution of the blocking temperatures (approximately below 50 K). The further kink on the ZFC curves around 200 K reveals the phase transition of the base liquid from solid to liquid state (liquefaction/freezing). The magnetizations measured at the FC regime (upper curves) decrease with increasing temperature confirming the typical pyromagnetic effect in ferrofluid MNP. The different magnitudes in both ZFC and FC magnetization curves reflect the different magnetic mass fraction (MNP concentration) in the measured ferrofluids.

From the locations of the ZFC shoulders around 50 K, it is estimated that the MNP size is around 10 nm. To determine the MNP size distribution experimentally, we prefer to analyze the magnetization curve measured at room temperature. We have applied the superposition of Langevin fitting functions on the magnetization curves [51]. With this method, one should bear in mind that the resulting sizes reflect the sizes of the magnetic cores without dead layers and surfactants. Thus, the mean magnetic diameter of MNP in the ferrofluids 1MOL, 2MOL, and 3MOL is found to be 11.1, 10.5, and 10.6 nm, respectively. Figure 3 shows the obtained nanoparticle size distribution for 1MOL ferrofluid.

The above-determined nanoparticle size distribution can be also deduced from the performed alternating current (ac) magnetic susceptibility measurements by Imego Dynomag, susceptometer, SE. The spectra of real and imaginary AC magnetic susceptibility are shown in Fig. 4. The imaginary susceptibility of each ferrofluid sample is near zero (overlapping curves) in the frequency range from 1 Hz to 100 kHz, meaning zero magnetic losses due to magnetic relaxations. The real parts of magnetic susceptibility exhibit quasiconstant behavior without observable dispersions in these frequencies. This behavior is a solid evidence of the well-relaxed nanoparticles in the oil with relaxation times (Brownian or Néel) occurring at frequencies above the high-frequency limit of the experiment. In general, the fast relaxation dynamics is the evidence of the individual nanoparticles of the above-presented size distribution with the absence of the MNP clusters.

The main experimental study reported herein was performed using MCR-502 rheometer from Physica Anton Paar GmbH equipped with the dielectric rheological device. The rheometer itself was first used to obtain viscosity and flow curves for each ferrofluid at three different temperatures. The shear rate-controlled tests were carried out with ascending steps from 1 s^{-1} to 1000 s^{-1}. Dielectric measurements of the ferrofluids were conducted using Agilent E4980A Precision LCR Meter with the basic impedance accuracy of 0.05%. Open and short corrections were performed before the measurements of the ferrofluids. The LCR meter with shielded wires was connected to the rheometer with the measuring system consisting of the dielectric cell P-PTD/DI and parallel plates PP/25/DI/TI with isolated geometry. A principal schematic representation of such a rheodielectric setup is published in Ref. [46]. The diameter of the circular plates is 25 mm and a measuring gap was set to 1 mm. The ferrofluid samples were sandwiched between the two plates simultaneously serving as a capacitor and a shearing geometry. The capacity of this plate capacitor with air is $C_0 = 9.9$ pF. An alternating electrical voltage of amplitude 20 Vrms over a frequency range from 20 Hz to 100 kHz was applied on the plates. The highest possible voltage amplitude was selected

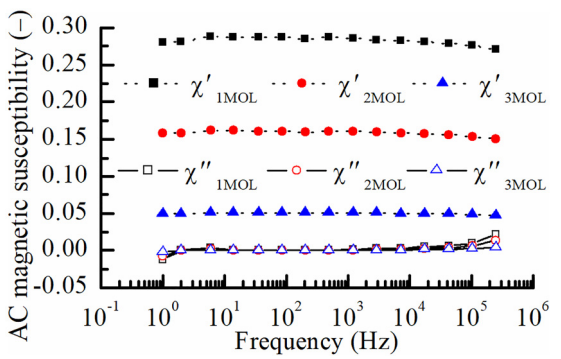

FIG. 4. Real (χ') and imaginary (χ") magnetic susceptibility spectra of the ferrofluids reflecting the small nanoparticle size with fast relaxation dynamics.

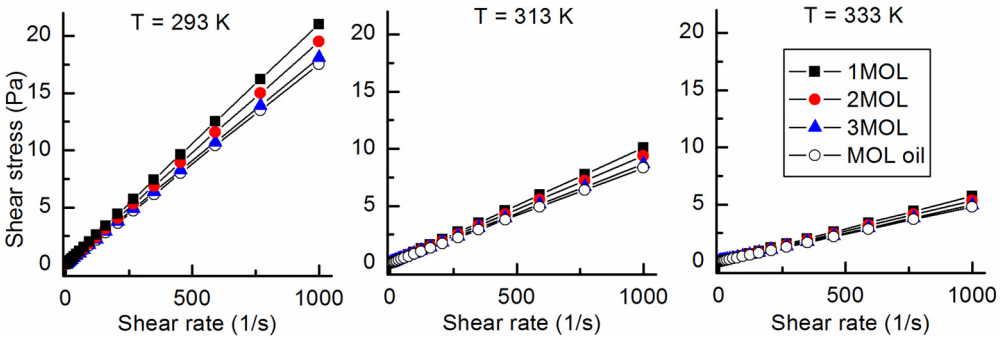

FIG. 5. The flow curves of the studied liquids measured at temperatures of 293, 313, and 333 K. The shown legend belongs to each graph.

purposely to get electric field intensity close to those present in electric power engineering electrical equipment. Then, dielectric spectra were recorded under the action of the top plate rotation, resulting in constant shear rates of 0, 10, 100, 500, and 1000 s^{-1}. With these shear rates, the measurements are conducted under laminar flow conditions. The rheodielectric measurements were performed at temperatures of 293, 313, and 333 K.

IV. RESULTS AND DISCUSSION

The obtained flow curves for the pure MOL oil and the three ferrofluid samples are presented in Fig. 5. There, the linear dependence of the shear stress on the shear rate shows that the viscosity of the oil and the ferrofluids remain constant across the entire measuring range, thus showing ideally viscous behavior (Newtonian behavior). It is clear that the viscosity increases with increasing MNP concentration and decreases with temperature. The particular viscosity values η_{avg} determined according to Eq. (8) are listed in Table II. The calculations were performed over the entire shear stress and shear rate range with subsequent averaging of the obtained viscosity values.

Figure 6 shows the cumulative representation of the real part of the dielectric permittivity of the three ferrofluids versus the frequency of the applied alternating electric voltage under the action of the set shear rates (0, 10 100, 500, and 1000 s^{-1}). At each temperature, the permittivity spectra have a plateau at the middle-frequency range, while at higher frequencies one observes a moderate permittivity decrease. A remarkable permittivity upturn (dielectric dispersion) appears at the low-frequency limit, below 100 Hz. This kind of permittivity behavior is a typical spectrum of a dielectric liquid containing conductive species (ions) [36,38–40]. As already reported in the literature, the source of the conductive species in the oil-based ferrofluid is associated with specific features of production and surface modification of MNP. The stabilization of MNP by oleic acid/oleate leads to different forms of interactions between the MNP surface ion and the carboxylic/carboxylate groups [38]. Moreover, a small amount of nonbonded oleic acid species is also present in the ferrofluid. Clearly, with increasing concentration of MNP one increases the polarizable and conductive species in the ferrofluid. As a result, the level of the permittivity spectrum shifts to higher values with increasing MNP concentration. On the other hand, with increasing temperature, the permittivity spectrum shifts to higher frequencies reflecting the shorter relaxation times due to the higher thermal energy and lower ferrofluid viscosity. This temperature-induced increase in the characteristic frequencies is better seen in dielectric spectra measured on ferrofluid thin layers [52]. Interestingly, the key message from Fig. 6 is that the spectra measured at the different shear rates overlap in a curve. Clearly, there is no measurable effect of the shear rate on the real permittivity spectrum. The detected deviations are observed only within an experimental error. This finding holds for measurements at each temperature.

The solid evidence of the dominating conductivity character of the ferrofluids' dielectric spectra is provided in the imaginary part of the complex permittivity in Fig. 7. This evidence is connected with Eq. (3) expressing the linear relation between the imaginary permittivity and DC conductivity, and the decreasing imaginary permittivity varying with f^{-1}. The linear fit with the slope of -1 is found for the spectrum of each ferrofluid. To keep the graph curves clear, we show the -1 slope only for 3MOL ferrofluid. From the presented imaginary permittivity spectra, one again observes that the spectra are shear rate independent.

Before discussing the shear rate independence of the low-frequency dielectric response of the ferrofluids, it is valuable to provide an insight into the ferrofluid's conductivity, which constitutes the dominating contribution to the revealed spectra. Firstly, we measured the ferrofluids' resistivity

TABLE II. The calculated dynamic viscosities of the studied liquids.

Sample	η_{avg} @ 293 K (mPa s)	η_{avg} @313 K (mPa s)	η_{avg} @333 K (mPa s)
1MOL	21.2	9.7	5.4
2MOL	19.5	8.9	5.1
3MOL	18.1	8.6	4.5
MOL oil	17.6	8.2	4.5

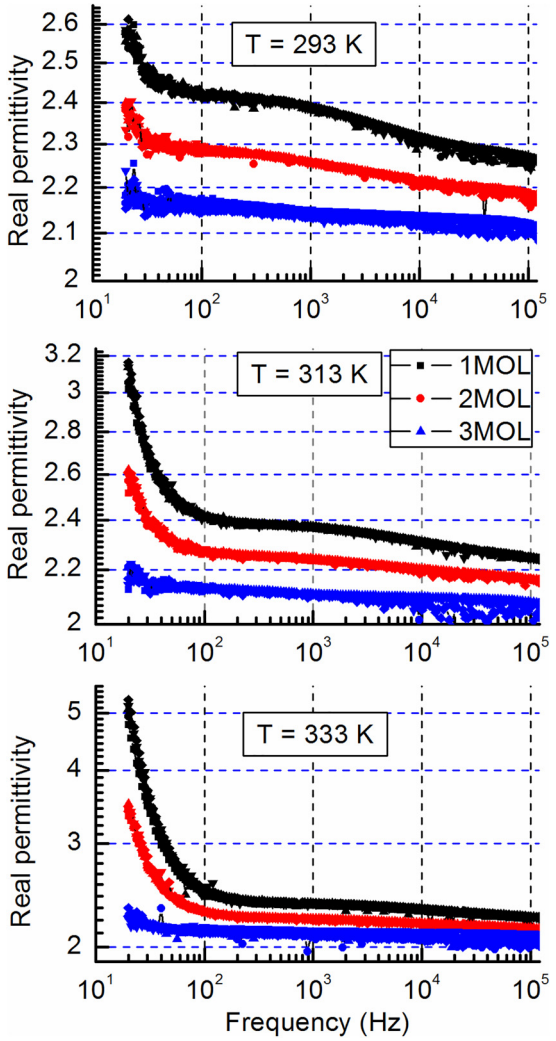

FIG. 6. The dielectric spectra of the real part of complex permittivity of the ferrofluids measured at three different temperatures and shear rates of 0, 10, 100, 500, and 1000 s^{-1}. The experimental data points are coincident for various shear rates. The spectra measured at the different shear rates overlap in a single curve.

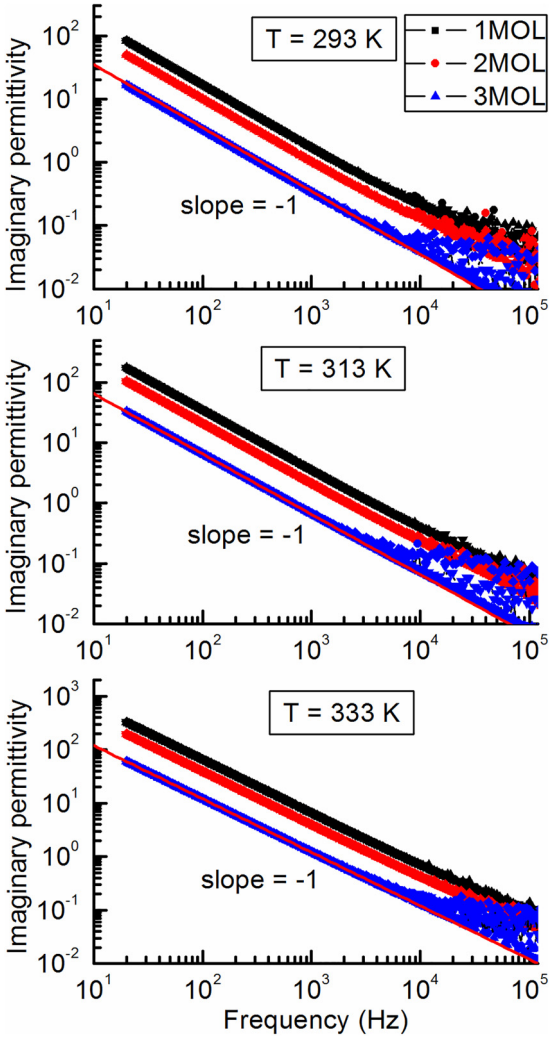

FIG. 7. The dielectric spectra of the imaginary part of complex permittivity of the ferrofluids measured at three different temperatures and shear rates of 0, 10, 100, 500, and 1000 s^{-1}. The spectra measured at the different shear rates overlap in a single curve. The line with the slope −1 emphasizes the conductivity contribution.

experimentally (Eltel ADTR-2K Plus) and then we took the inverse of the resistivity values to obtain the DC conductivity. The resistivity of the ferrofluids and the pure oil at the three temperatures is shown in Fig. 8(a). The DC conductivity of the liquids is presented in Fig. 8(b).

As Fig. 8(a) shows, the resistivity of ferrofluid samples (light Y axis) is four orders of magnitude lower than the resistivity of the oil (right Y axis). The resistivity of each sample decreases with increasing temperature. Moreover, the ferrofluid with the highest MNP concentration (1MOL) has such a low resistivity at 330 K that it is beyond the available measuring range of the employed device. In the inverse representation, one understands that the ferrofluid DC conductivity increases with temperature and it is four orders of magnitude greater than that of the transformer oil [Fig. 8(b)]. The increase in conductivity with temperature reflects the motion of ions through the viscous transformer oil of viscosity η. It is well-known that the electric force exerted by the applied electric field between the two disk electrodes is balanced by a viscous force (Stokes law) and it can be written as

$$qE = 6\pi\eta R v_d, \tag{9}$$

where q is the ion charge, E is the field intensity, R is the ion radius, and v_d is the ion drift velocity. Then, according to Walden's rule, the ion mobility is defined as follows:

$$\mu_{\text{ion}} = q/6\pi\eta R. \tag{10}$$

The temperature dependence of ionic mobilities in nonpolar liquids follows an Arrhenius-type dependence

$$\mu_{\text{ion}} = \mu_0 e^{-W/kT} \tag{11}$$

with W and kT denoting the activation and thermal energy, respectively, and the DC conductivity is in linear relation with the ionic mobility

$$\sigma = nq\mu_{\text{ion}}, \tag{12}$$

where n denotes the concentration of ions [53]. As mentioned above, the concentration of ions increases with increasing

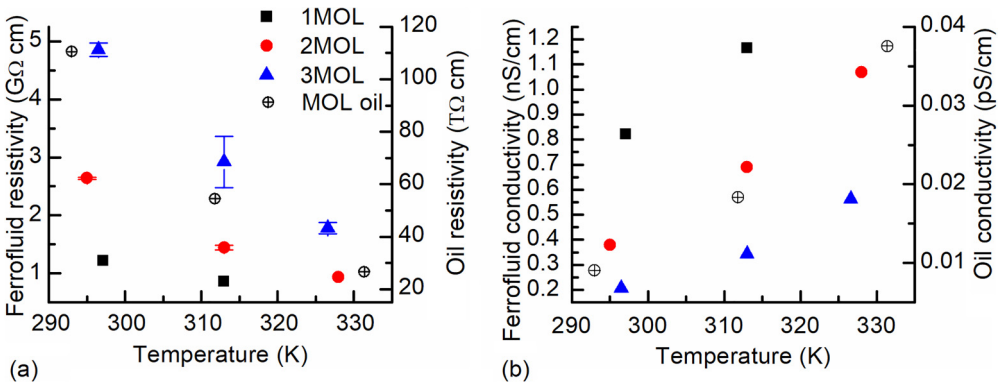

FIG. 8. Resistivity of ferrofluids (left Y axis) and the pure transformer oil (right Y axis) measured at three different temperatures (a). Direct current (DC) conductivity of ferrofluids (left Y axis) and the pure transformer oil (right Y axis) at three different temperatures (b).

MNP concentration and that is why the DC conductivity increases with MNP concentration. Our further discussion of the shear-independent dielectric response (Figs. 6 and 7), with the dominating conductivity contribution is based on the given general considerations on ion mobility in nonpolar liquids.

The directed ion motion in ferrofluids, as a response to the applied voltage, leads to the accumulation of ions at the electrode surfaces. The speed of that response, resulting in the charging of the electrodes, can be expressed by the well-known time constant (τ_C), given by a product of the capacity of the capacitor C_0 and the ohmic resistance R_e in units of Ω. The ohmic resistance can be easily calculated as $R_e = \rho/4r_0$, where ρ is the measured resistivity and r_0 is the radius of the disk electrode. Thus, using the values in Fig. 8(a), we calculated the time constants for the ferrofluids charging the electrode surfaces at three different temperatures. The obtained results are presented in Fig. 9(a). The values of the time constants are in the range of tens of seconds, exhibiting a decrease with increasing temperatures. The shortest time constants are found for the ferrofluid of the highest MNP concentration (1MOL), while the ferrofluid with the lowest MNP concentration (3MOL) exhibits the longest time constants. Nevertheless, in each case, the time scale is in the range of tens of seconds and that seems to be a clue to the explanation of the low-frequency dielectric dispersion (upturn) in Fig. 6. The process emerging at the low-frequency limit is driven by the conductivity and leads to the electrode polarization, or the double layer charging of the electrodes. In order to express the process in the frequency domain, we calculate the inverse of the time constants, obtaining the characteristic frequencies of the electrode surface charging by the migrating ions. The characteristic frequencies are displayed in Fig. 9(b). One can see that the characteristic frequencies are in the range of hundredths of Hz, the range which is below our available measuring frequencies. However, the low-frequency dielectric behavior shown in Figs. 6 and 7 clearly indicates the calculated frequency range of the observed process.

One can therefore see that the slow dielectric relaxations in the ferrofluids, represented by ion migration, are not influenced by the applied shear conditions. In our experiments, the upper electrode rotates, and the upper ferrofluid layer is exposed to the shear stress resulting in the shear gradient (up to $1000\,s^{-1}$) in the ferrofluid sandwiched between the rotating and the static disk electrode. At the same time, owing to the applied AC voltage, the ions migrate towards the electrodes, i.e., in the same direction as the shear gradient. Considering the applied shear rates and the gap width between the electrodes, one finds that the maximal flow velocity is 1 m/s. Based on a simple and classical theoretical approach, one can also determine both, the applied shear force and the acting electric force quantitatively. Following Eq. (6), and substituting the plate area and the maximal value of the applied shear stress in our experiments (21 Pa for 1MOL and $1000\,s^{-1}$ at 293 K), we find the maximal shear force

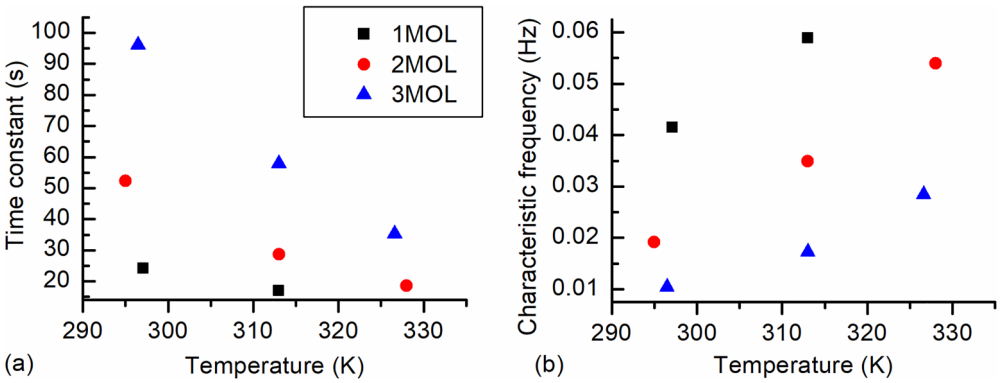

FIG. 9. The temperature-dependent time constant (a) and characteristic frequency (b) for the charging the electrode-ferrofluid interface.

at the level of 1×10^{-2} N. On the other hand, from the capacity of the capacitor one can determine the total electric charge stored in the capacitor filled with a particular sample. Then, the product of the charge and the electric field intensity in the capacitor (20 kV/m) yields the electric force acting on the charge. When considering the maximal capacity (approx. 25 pF) measured for 1MOL at 293 K and 20 Hz, one gets the maximal charge approx. 0.5 nC, and the maximal electric force is at the level of 1×10^{-5} N. The applied shear force is therefore three orders of magnitude greater than the electric force. However, it is evident from the performed experiments (Figs. 6 and 7) that the significantly greater shear force does not influence the ion migration towards the rotating electrode and the interfacial ferrofluid layer flow has no impact on the ferrofluid dielectric response. Under the set experimental conditions, the ions migrate across the shear flow velocity in the shear rate direction and the given rheological conditions do not affect the slow (low-frequency) dielectric process. The confirmed shear rate-independent dielectric response of the transformer oil-based ferrofluids is of practical importance when considering ferrofluids as dielectric media in electrical equipment with the presence of electric forces and natural or forced convection (e.g., power transformers). In this type of ferrofluid application, it is crucial to insure the stability of the dielectric properties under flow conditions. The dielectric response of the studied ferrofluids under the examined conditions is therefore shear rate-independent.

V. CONCLUSION

Transformer oil-based ferrofluids with noninteracting magnetic nanoparticles were subjected to rheodielectric investigation. The low-frequency dielectric spectra of ferrofluids with various nanoparticle concentrations show remarkable conductivity contribution leading to the electrode polarization. Nonbonded oleic acid and residual ions from nanoparticle preparation and stabilization are considered to be the main source of the mobile charge in the ferrofluids. The DC electrical conductivity of the ferrofluids was found experimentally and employed in the determination of time constants for charging of the electrode surface. The process takes place in the time scale of tens of seconds, therefore at frequencies of hundredths of Hz. It is found that this slow dielectric relaxation process is shear rate independent. The low-frequency dielectric spectra measured under various shear rates overlap within a single curve with variations within the experimental error. Under the set up shear flow geometry, the ions migrate across the shear flow velocity in the shear rate direction and the given rheological conditions do not affect the slow dielectric process. It is experimentally proven that the electrical forces dominate the ion motion in the ferrofluids over the shear forces. Based on the conducted experiments, one can also conclude that there are no shear-induced structural changes in the ferrofluids, the presence of which would influence the dielectric response. The finding of the stable dielectric response of ferrofluids under the shear flow conditions supports the application of ferrofluids as dielectric media in electrical equipment.

ACKNOWLEDGMENTS

This research was funded by Slovak Research and Development Agency under Contracts No. APVV-22–0115, No. APVV-18–0160, No. APVV-22–0060, and Slovak Academy of Sciences and Ministry of Education in the framework of Projects VEGA No. 2/0029/24, No. 1/0353/22, No. 1/0380/24 and the Cultural and Educational Grant Agency of the Ministry of Education, Research, Development and Youth of the Slovak Republic under Contract No. 008TUKE-4/2019. The work also received support from REA.A – Marie Skłodowska-Curie Actions & Support to Experts within the Projects No. 101182948 — RETROTRAFO — HORIZON-MSCA-2023-SE-01, and Project No. NFP ITMS Code 313011T557“ (Project No. 019/2019/1.1.3/OPVaI/DP with ITMS Code 313011T557 titled ”Support of the Research and Development Potential in the Area of Transportation Vehicles.

DATA AVAILABILITY

The data that support the findings of this article are not publicly available. The data are available from the authors upon reasonable request.

[1] R. E. Rosensweig, *Ferrohydrodynamics* (Dover Publications, New York, 2013).
[2] A. Kumar and S. Subudhi, Heat Mass Transf. **54**, 241 (2018).
[3] O. Oehlsen, S. I. Cervantes-Ramírez, P. Cervantes-Avilés, and I. A. Medina-Velo, ACS Omega **7**, 3134 (2022).
[4] A. Mertelj, L. Cmok, and M. Čopič, Phys. Rev. E **79**, 041402 (2009).
[5] J. A. Miranda, R. M. Oliveira, and D. P. Jackson, Phys. Rev. E **70**, 036311 (2004).
[6] P. Ilg, M. Kröger, and S. Hess, Phys. Rev. E **71**, 051201 (2005).
[7] A. Sreekumari and P. Ilg, Phys. Rev. E **92**, 012306 (2015).
[8] Z. Li, Y. Guo, H. Wang, C. Deng, J. Dong, and Z. Song, Magnetochemistry. **9**, 143 (2023).
[9] B. J. de Gans, C. Blom, A. P. Philipse, and J. Mellema, Phys. Rev. E **60**, 4518 (1999).
[10] D. N. Chirikov, S. P. Fedotov, L. Y. Iskakova, and A. Y. Zubarev, Phys. Rev. E **82**, 051405 (2010).
[11] D. N. Chirikov and A. Y. Zubarev, Colloid J. **85**, 87 (2023).
[12] H. C. Weng, C. L. Chen, and C. K. Chen, Phys. Rev. E **78**, 056305 (2008).
[13] A. Gómez, A. Barón, J. Berasategi, M. Blanco, A. García, J. Gutiérrez, D. Iglesias-Rojas, M. Insausti, S. Lanceros-Mendez, C. R. Tubio, and M. M. Bou-Ali, J. Magn. Magn. Mater. **593**, 171881 (2024).
[14] W. Li, Z. Li, W. Han, Y. Li, S. Yan, Q. Zhao, and F. Chen, Phys. Fluids **35**, 012002 (2023).
[15] R. V. Upadhyay, K. Parekh, and K. Raj, J. Magn. Magn. Mater. **586**, 171206 (2023).
[16] C. Yang, Y. Jiang, T. Li, X. Wang, P. Cheng, and Y. Li, J. Mol. Liq. **399**, 124419 (2024).

[17] I. D. O. Pereira and F. R. Cunha, Phys. Fluids **35**, 112008 (2023).
[18] R. E. Rosensweig, Science **271**, 614 (1996).
[19] J.-C. Shih and H.-Y. Chu, Phys. Fluids **34**, 014103 (2022).
[20] M. D. Contreras-Mateus, A. Chaves-Guerrero, N. N. Nassar, and F. H. Sánchez, Phys. Fluids **36**, 043115 (2024).
[21] Y. Lv, M. Rafiq, C. Li, and B. Shan, Energies **10**, 1025 (2017).
[22] M. S. Pattanaik, V. B. Varma, S. K. Cheekati, V. Chaudhary, and R. V. Ramanujan, Sci. Rep. **11**, 24167 (2021).
[23] J. Kurimsky, M. Rajnak, R. Cimbala, K. Paulovicova, Z. Rozynek, P. Kopcansky, and M. Timko, J. Mol. Liq. **325**, 115244 (2021).
[24] M. Rajňák, M. Franko, K. Paulovičová, M. Karpets, K. Parekh, R. Upadhyay, J. Kurimský, B. Dolník, R. Cimbala, P. Havran, M. Timko, and P. Kopčanský, J. Phys. D **55**, 345002 (2022).
[25] M. Rajnak, V. I. Petrenko, M. V. Avdeev, O. I. Ivankov, A. Feoktystov, B. Dolnik, J. Kurimsky, P. Kopcansky, and M. Timko, Appl. Phys. Lett. **107**, 073108 (2015).
[26] M. Karpets, M. Rajnak, V. Petrenko, I. Gapon, M. Avdeev, L. Bulavin, M. Timko, and P. Kopcanský, J. Mol. Liq. **362**, 119773 (2022).
[27] M. Rajnak, M. Timko, P. Kopcansky, K. Paulovicova, J. Tothova, J. Kurimsky, B. Dolnik, R. Cimbala, M. V. Avdeev, V. I. Petrenko, and A. Feoktystov, J. Magn. Magn. Mater. **431**, 99 (2017).
[28] A. Spanoudaki and R. Pelster, J. Magn. Magn. Mater. **252**, 71 (2002).
[29] M. M. Rădulescu, J. Magn. Magn. Mater. **85**, 144 (1990).
[30] C. N. Marin, I. Malaescu, and A. Savici, Acta Phys. Pol. A, **124**, 724 (2013).
[31] I. Malaescu and C. N. Marin, J. Magn. Magn. Mater. **252**, 68 (2002).
[32] C. N. Marin, P. C. Fannin, I. Malaescu, and G. Matu, Phys. Lett. A **384**, 126786 (2020).
[33] P. Havran, R. Cimbala, J. Király, M. Rajňák, S. Bucko, J. Kurimský, and B. Dolník, Process. **10**, 2405 (2022).
[34] M. Timko, K. Marton, L. Tomco, J. Kiraly, M. Molcan, M. Rajnak, P. Kopcansky, R. Cimbala, F. Stoian, S. Holotescu, and A. Taculescu, Magnetohydrodynamics **48**, 427 (2012).
[35] M. Rajnak, B. Dolnik, J. Krempasky, R. Cimbala, K. Parekh, R. Upadhyay, K. Paulovicova, P. Kopcansky, and M. Timko, J. Phys. **54**, 035303 (2020).
[36] M. Rajnak, Z. Spitalsky, B. Dolnik, J. Kurimsky, L. Tomco, R. Cimbala, P. Kopcansky, and M. Timko, Phys. Rev. Appl. **11**, 024032 (2019).
[37] F. Batalioto, E. S. Gonçalves, A. M. F. Neto, and G. Barbero, J. Electroanal. Chem. **874**, 114452 (2020).
[38] F. Batalioto, G. Barbero, A. F. C. Campos, and A. M. Figueiredo Neto, Phys. Chem. Chem. Phys. **23**, 2819 (2021).
[39] F. Batalioto, A. M. Figueiredo Neto, and G. Barbero, Phys. Chem. Chem. Phys. **24**, 3400 (2022).
[40] F. Batalioto, K. Parekh, G. Barbero, and A. M. Figueiredo Neto, J. Appl. Phys. **136**, 94701 (2024).
[41] F. Batalioto, M. Chand, A. F. C. Campos, J. Depeyrot, G. Barbero, and A. M. F. Neto, Phys. Chem. Chem. Phys. **24**, 28506 (2022).
[42] S. Capaccioli, D. Prevosto, A. Best, A. Hanewald, and T. Pakula, J. Non. Cryst. Solids **353**, 4267 (2007).
[43] Y. Peng, Y. M. Shkel, and G. Kim, J. Rheol. (N Y) **49**, 297 (2005).
[44] K. Negita and H. Kaneko, Phys. Rev. E **80**, 011705 (2009).
[45] D. Steinhauser, M. Möwes, and M. Klüppel, J. Phys. Condens. Matter **28**, 495103 (2016).
[46] C. Misra, P. Gadige, and R. Bandyopadhyay, J. Colloid Interface Sci. **630**, 223 (2023).
[47] I. Popov, S. Cheng, and A. P. Sokolov, *Macromolecular Engineering: From Precise Synthesis to Macroscopic Materials and Applications* (Wiley, New York, 2022), pp. 1–39.
[48] A. Schönhals and F. Kremer, in *Broadband DielectrIc Spectroscopy* (Springer, Berlin, 2003), pp. 1–33.
[49] Thomas G. Mezger, *The Rheology Handbook: For Users of Rotational and Oscillatory Rheometers* (Vincentz Network, Hannover, Germany, 2020).
[50] L. Vékás, D. Bica, and M. V. Avdeev, China Particuology **5**, 43 (2007).
[51] Z. Rozynek, A. Józefczak, K. D. Knudsen, A. Skumiel, T. Hornowski, J. O. Fossum, M. Timko, P. Kopčanský, and M. Koneracká, Eur. Phys. J. E **34**, 28 (2011).
[52] M. Rajnák, J. Kurimský, B. Dolník, R. Cimbala, K. Paulovicová, P. Kopcanský, and M. Timko, Acta Phys. Pol. A **131**, 943 (2017).
[53] R. Bartnikas and A. S. T. M. International., *Electrical Insulating Liquids* (ASTM, New York, 1994).